Available online at www.sciencedirect.com
SCIENCE DIRECT®
Journal of Solid State Chemistry 177 (2004) 2158–2167
JOURNAL OF SOLID STATE CHEMISTRY
http://elsevier.com/locate/jssc

Phase formation in the systems Ag_2MoO_4–MO–MoO_3 (M = Ca, Sr, Ba, Pb, Cd, Ni, Co, Mn) and crystal structures of $Ag_2M_2(MoO_4)_3$ (M = Co, Mn)

G.D. Tsyrenova,[a,*] S.F. Solodovnikov,[b] E.G. Khaikina,[a] E.T. Khobrakova,[a] Zh.G. Bazarova,[a] and Z.A. Solodovnikova[b]

[a] *Baikal Institute of Nature Management, Siberian Branch, Russian Academy of Sciences, Sakh'ynova St. 6, Ulan-Ude 670047, Buryat Republic, Russia*
[b] *Nikolaev Institute of Inorganic Chemistry, Siberian Branch, Russian Academy of Sciences, Akad. Lavrent'ev Ave. 3, Novosibirsk 630090, Russia*

Received 5 September 2003; received in revised form 8 January 2004; accepted 14 January 2004

Abstract

Phase equilibria in the systems $Ag_2MoO_4-MMoO_4$ (M = Ca, Sr, Ba, Pb, Ni, Co, Mn) and subsolidus phase relations in the systems $Ag_2MoO_4-MO-MoO_3$ (M = Ca, Pb, Cd, Mn, Co, Ni) were investigated using XRD and thermal analysis. The systems $Ag_2MoO_4-MMoO_4$ (M = Ca, Sr, Ba, Pb, Ni) belong to the simple eutectic type whereas in the systems $Ag_2MoO_4-MMoO_4$ (M = Co, Mn) incongruently melting $Ag_2M_2(MoO_4)_3$ (M = Co, Mn) were formed. In the ternary oxide systems studied no other compounds were found. Low-temperature LT-$Ag_2Mn_2(MoO_4)_3$ reversibly converts into the high-temperature form of a similar structure at 450–500°C. The single crystals of $Ag_2Co_2(MoO_4)_3$ and LT-$Ag_2Mn_2(MoO_4)_3$ were grown and their structures determined (space group $P\bar{1}$, $Z = 2$; lattice parameters are $a = 6.989(1)$ Å, $b = 8.738(2)$ Å, $c = 10.295(2)$ Å, $\alpha = 107.67(2)°$, $\beta = 105.28(2)°$, $\gamma = 103.87(2)°$ and $a = 7.093(1)$ Å, $b = 8.878(2)$ Å, $c = 10.415(2)$ Å, $\alpha = 106.86(2)°$, $\beta = 105.84(2)°$, $\gamma = 103.77(2)°$, respectively) and refined to $R(F) = 0.0313$ and 0.0368, respectively. The both compounds are isotypical to $Ag_2Zn_2(MoO_4)_3$ and contain mixed frameworks of MoO_4 tetrahedra and pairs of $M^{2+}O_6$ octahedra sharing common edges. The Ag^+ ions are disordered and located in the voids forming infinite channels running along the a direction. The peculiarities of the silver disorder in the structures of $Ag_2M_2(MoO_4)_3$ (M = Zn, Mg, Co, Mn) are discussed as well as their relations with analogous sodium-containing compounds of the structural family of $Na_2Mg_5(MoO_4)_6$. The phase transitions in $Ag_2M_2(MoO_4)_3$ (M = Mg, Mn) of distortive or order–disorder type are suggested to have superionic character.

Keywords: Molybdates; Silver; Bivalent metals; Phase relations; Phase transition; Crystal structure; Cation disorder

1. Introduction

During the last four decades numerous double molybdates of bivalent metals and alkaline elements, copper(I) or thallium(I) with general formula $A^+_{2m}M^{2+}_n(MoO_4)_{m+n}$ have been obtained and intensively explored [1–22]. Crystal chemistry of these compounds has been studied in detail [3,5,12–14,20,22]. A number of the compounds possess distortive and order–disorder type phase transitions, ferro/piezo activity and high ionic conductivity [20,23–31]. The last property was found for nonstoichiometric lithium and sodium-containing double molybdates where mobile Li^+ and Na^+ cations are located in channels of mixed frameworks of MoO_4 tetrahedra and $(M^{2+}, A^+)O_6$ octahedra [20].

Ionic conductivity may also be expected for analogous silver-containing double molybdates. Unfortunately, literature data on the interaction in the systems $Ag_2MoO_4-MMoO_4$ are restricted so far by papers [32–34] only. Gicquel-Mayer et al. [32] prepared single crystals of $Ag_2Zn_2(MoO_4)_3$ and determined its structure. Recently, we constructed the phase diagram of the system Ag_2MoO_4–$CdMoO_4$ [33], studied phase formation in the system Ag_2O–MgO–MoO_3, and determined the crystal structure of a novel double molybdate $Ag_2Mg_2(MoO_4)_3$ [34].

*Corresponding author. Fax: +3012-434753.
E-mail address: gtsyr@binm.baikal.net (G.D. Tsyrenova).

0022-4596/$ - see front matter © 2004 Published by Elsevier Inc.
doi:10.1016/j.jssc.2004.01.002

The objects of this work are (a) to investigate phase equilibria in the systems $Ag_2MoO_4-MMoO_4$ (M = Ca, Sr, Ba, Pb, Ni, Co, Mn); (b) to study phase formation in subsolidus areas of the systems $Ag_2MoO_4-MO-MoO_3$ (M = Ca, Pb, Cd, Mn, Co, Ni), and (c) to determine the crystal structures of double molybdates formed in the systems above.

2. Experimental

2.1. Synthesis

The cubic form of silver molybdate was prepared by step annealing of stoichiometric mixture of $AgNO_3$ and MoO_3 (both reagent grade) for 50 h at 250°C to 450°C. The phase transition of Ag_2MoO_4 at 482°C observed in [35] was not fixed with thermal analysis though upon heating a powder sample changed its color in the same way as described by these authors. The melting point of Ag_2MoO_4 is 575°C and the unit cell parameter is close to that cited in [36].

Molybdates $MMoO_4$ (M = Ca, Sr, Ba, Cd, Pb, Ni, Co, Mn) was synthesized by solid-state reactions from carbonates or oxides of bivalent metals and molybdenum trioxide (all reagent grade) following to recommendations of [37,38]. The powder diffraction patterns and the thermal constants of the molybdates prepared agree well with data of ICDD PDF-2 and the results of [38].

The reaction mixtures for studying subsolidus phase relations and constructing $T-x$ phase diagrams of the systems $Ag_2MoO_4-MMoO_4$ were prepared with step of 5 mol%, while in the vicinity of the initial components and the compositions of the proposed intermediate phases the step was 1–2 mol%. The subsolidus phase relations of $Ag_2MoO_4-MO-MoO_3$ systems were determined by the "intersecting joins" method [39].

Single crystals of double molybdates were grown by spontaneous crystallizations from nonstoichiometric melts. The temperature was kept automatically with an accuracy of $\pm 0.5°$. The cooling rate was varied from 40°C/h to 1°C/h.

2.2. X-ray diffraction and structure determination

Monitoring of solid-state synthesis and phase equilibration was carried out by X-ray powder diffraction (XRD) with a DRON-UM1 diffractometer using Ni-filtered Cu$K\alpha$ radiation. In order to refine the compositions and homogeneity ranges of intermediate phases, powder diffraction patterns of some samples were recorded with an Enraf-Nonius FR-552 focusing camera using Cu$K\alpha_1$ radiation and Ge as an internal standard. The lattice parameters were refined by least-squares method with the CSD program package [40].

X-ray diffraction data for structure determination of $Ag_2M_2(MoO_4)_3$ (M = Co, Mn) were collected with graphite-monochromated Mo$K\alpha$ radiation ($\lambda = 0.71073$ Å) on an Enraf-Nonius CAD-4 diffract-

Table 1
Crystal data and structure refinement results for $Ag_2M_2(MoO_4)_3$ (M = Co, Mn)

Formula	$Ag_2Co_2(MoO_4)_3$	LT-$Ag_2Mn_2(MoO_4)_3$
Formula weight (g/mol)	813.42	805.44
Crystal system	Triclinic	Triclinic
Space group	$P\bar{1}$	$P\bar{1}$
Unit cell dimensions		
	$a = 6.989(1)$ Å	$a = 7.093(1)$ Å
	$b = 8.738(2)$ Å	$b = 8.878(2)$ Å
	$c = 10.295(2)$ Å	$c = 10.415(2)$ Å
	$\alpha = 107.67(2)°$	$\alpha = 106.86(2)°$
	$\beta = 105.28(2)°$	$\beta = 105.84(2)°$
	$\gamma = 103.87(2)°$	$\gamma = 103.77(2)°$
V (Å^3); Z	541.8(2); 2	566.9(2); 2
Calculated density (g/cm^3)	4.986	4.719
Crystal size (mm)	$0.06 \times 0.09 \times 0.40$	$0.10 \times 0.26 \times 0.44$
Absorption coefficient (m/m)	9.941	8.803
θ range (deg) for data collection	2.23–29.96	2.20–34.96
Miller index ranges	$-7 \leqslant h \leqslant 0$, $-11 \leqslant k \leqslant 12$, $-13 \leqslant l \leqslant 14$	$-11 \leqslant h \leqslant 0$, $-13 \leqslant k \leqslant 14$, $-16 \leqslant l \leqslant 16$
Reflections collected/unique	2841/2628	5109/4800
	(R(int) = 0.0252)	(R(int) = 0.0195)
Number of parameters	196	196
Goodness-of-fit on F^2 (GOF)	0.982	1.129
Final R indices ($I > 2\sigma(I)$)	$R(F) = 0.0313$, w$R(F^2) = 0.0775$	$R(F) = 0.0368$, w$R(F^2) = 0.1055$
R indices (all data)	$R(F) = 0.0378$, w$R(F^2) = 0.0792$	$R(F) = 0.0410$, w$R(F^2) = 0.1075$
Extinction coefficient	0.0251(7)	0.0079(7)
Largest difference peak and hole (e/Å^3)	1.689 and −1.568	2.923 and −2.207

ometer at room temperature using standard techniques. Intensity data were measured using $\theta/2\theta$ scans with variable speed (ω range (deg.) $= 0.9 + 0.35\tan(\theta)$). An empirical absorption correction was applied by measuring four azimuthal scan curves. The structures were solved by direct methods (XS) and refined by full-matrix least-squares method on F^2 in anisotropic approximation with SHELX-97 Release 97-2 package [41]. The crystal data, experimental and refinement results of $Ag_2M_2(MoO_4)_3$ (M = Co, Mn) are summarized in Table 1.

2.3. Thermal analysis and density measurements

Thermal analytical study was carried out with a MOM OD-103 derivatograph (Pt–Pt/Rh thermocouple, heating rate 10°C/min). For a number of the intermediate samples melting effects were weak and the liquidus curve, as a rule, was determined visually using a POLAM-211C polarizing microscope with a hot stage allowing to observe phase transformations up to 1000°C. The sample was placed into a platinum loop heating with alternative current at a rate 5°C/min to 100°C/min. Temperature of the samples were determined according to the calibration curve plotted using melting temperatures of well-documented reference materials.

The densities of samples were determined pycnometrically in CCl_4 at 25°C.

3. Results and discussion

3.1. The systems Ag_2MoO_4–$MMoO_4$ (M=Ca, Sr, Ba, Pb, Ni, Co, Mn)

According to the character of the phase relations, the systems $Ag_2MoO_4-MMoO_4$ (M = Ca, Sr, Ba, Pb, Ni, Co, Mn) can be divided into two groups: (i) without phase formation (simple eutectic type) and (ii) with formation of an intermediate compound.

The simple eutectic type of interaction type is primarily observed in systems involving molybdates of bivalent cations (Ca, Sr, Ba, Pb, Cd), which crystallize in the structure of scheelite $CaWO_4$. $T-x$ phase diagrams of the systems $Ag_2MoO_4-MMoO_4$ (M = Ca, Pb) are presented in Figs. 1a and b. The coordinates of the eutectic point in the system with calcium molybdate are 560°C and 5 mol% $CaMoO_4$. The eutectic mixture in the Ag_2MoO_4–$PbMoO_4$ system contains 10 mol% $PbMoO_4$ and melts at 540°C. Earlier we established the simple eutectic type for the phase diagram of the system Ag_2MoO_4–$CdMoO_4$ [33] as well. In the systems $Ag_2MoO_4-MMoO_4$ (M = Sr, Ba), no intermediate phases were also fixed from XRD data.

The simple eutectic type of interaction was also observed in the system Ag_2MoO_4–$NiMoO_4$ (Fig. 1c). The eutectic mixture melts at 550°C and contains 6 mol% $NiMoO_4$. DTA curves show the phase transition of $NiMoO_4$ at 640°C in the region near this compound.

In the specimens of the system Ag_2MoO_4–$CoMoO_4$ annealed at 500°C we found the compound $Ag_2Co_2(MoO_4)_3$ which melts incongruently at 630°C (Fig. 2a). The coordinates of eutectic point are 550°C and 15 mol% $CoMoO_4$. The peritectic point corresponds to 22 mol% $CoMoO_4$. In the samples with a large content of cobalt molybdate, the endothermic effect is observed at 480°C that was referred to the phase transformation of $CoMoO_4$.

According to literature data [42], $NiMoO_4$ and $CoMoO_4$ possess a similar polymorphism. At atmospheric pressure the both compounds are dimorphic, their low-temperature forms belong to the structure type of α-$CoMoO_4$ and upon heating (640°C for nickel molybdate and 480°C for cobalt molybdate, respectively) they are reversibly transformed into the high-temperature modifications with the structure of α-$MnMoO_4$.

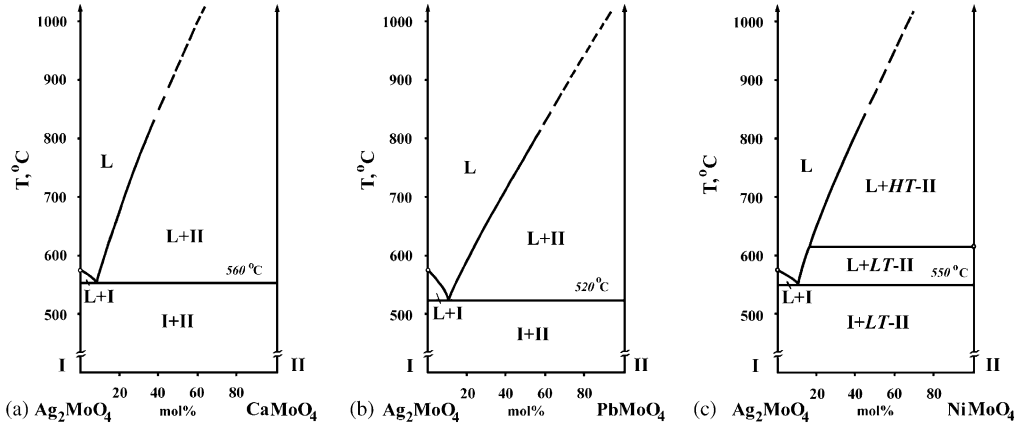

Fig. 1. $T-x$ phase diagrams of the systems $Ag_2MoO_4-MMoO_4$: (a) $Ag_2MoO_4-CaMoO_4$; (b) $Ag_2MoO_4-PbMoO_4$; (c) $Ag_2MoO_4-NiMoO_4$.

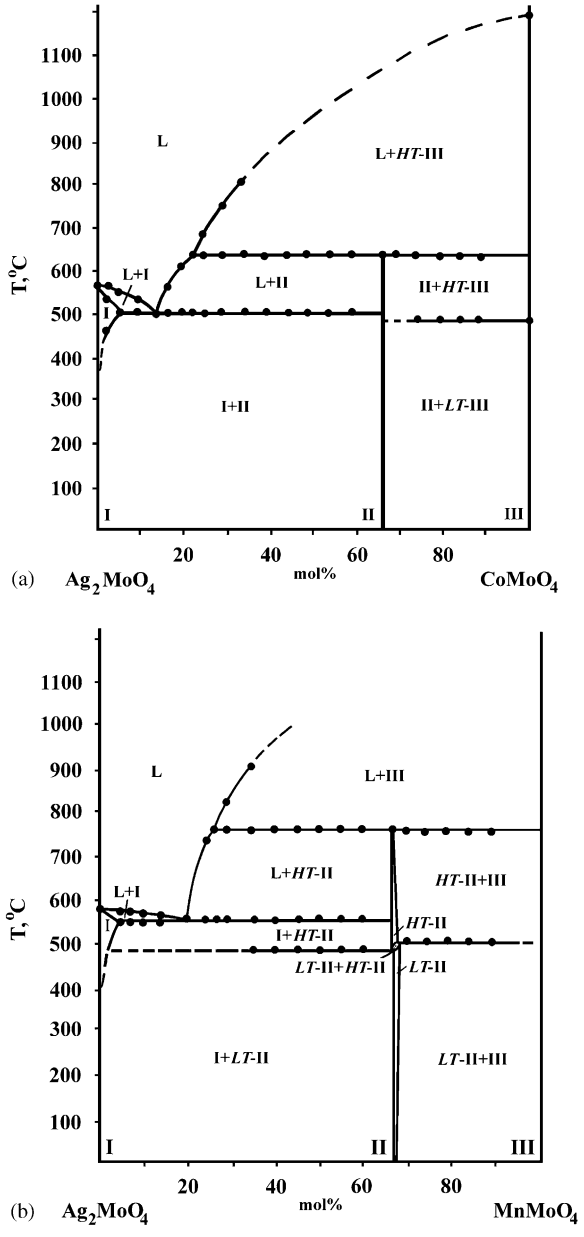

Fig. 2. $T-x$ phase diagrams of the systems $Ag_2MoO_4-MMoO_4$ (M=Co, Mn): (a) $Ag_2MoO_4-CoMoO_4$; (b) $Ag_2MoO_4-MnMoO_4$. I—Ag_2MoO_4; II—$Ag_2M_2(MoO_4)_3$; III—$MMoO_4$.

An essential difference in temperatures of the phase transitions of $MMoO_4$ (M=Ni, Co) may be a reason that no phase like $Ag_2Co_2(MoO_4)_3$ forms in the nickel-containing system. In our opinion, the formation of $Ag_2Co_2(MoO_4)_3$ is a result of the interaction of Ag_2MoO_4 and high-temperature form of $CoMoO_4$ initiated by loosening the crystal lattice of cobalt molybdate upon its polymorphous transformation. In the system Ag_2MoO_4–$NiMoO_4$, the samples melt below the temperature of the phase transition in nickel molybdate.

The phase diagram of the system Ag_2MoO_4–$MnMoO_4$ is given in Fig. 2b. It also characterized by the formation of the compound 1:2 and the presence of one eutectic (560°C and 20 mol% $MnMoO_4$) and one peritectic (760°C and 25 mol% $MnMoO_4$) points. XRD data show that the reaction between the simple molybdates starts at 350–400°C. Single-phase $Ag_2Mn_2(MoO_4)_3$ was obtained by annealing the stoichiometric mixture of simple molybdates at 500°C for 150 h. It reversibly converts into the high-temperature form at 450–500°C. Double molybdate $Ag_2Mg_2(MoO_4)_3$ behaves similarly [34]. The temperature dependence of the phase transformation on the reaction mixture composition allowed to suggest for this compound a small homogeneity region expanding to $MnMoO_4$. Its range at room temperature can be estimated ca. 1 mol% (at 500°C ca. 2 mol%).

Single crystals of $Ag_2Co_2(MoO_4)_3$ and LT-$Ag_2Mn_2(MoO_4)_3$ were prepared by spontaneous crystallization of nonstoichiometric melts. The crystals suitable for X-ray structure determination were obtained by crystallization of the mixtures 82 mol% Ag_2MoO_4 + 18 mol% $CoMoO_4$ and 77 mol% Ag_2MoO_4 + 23 mol% $MnMoO_4$ at slow cooling (in the range 600–200°C and 750–200°C, respectively). We found $Ag_2Co_2(MoO_4)_3$ and low-temperature LT-$Ag_2Mn_2(MoO_4)_3$ crystallizing in the triclinic system (space group $P\bar{1}$, $Z=2$) and being isostructural to $Ag_2M_2(MoO_4)_3$ (M=Zn, Mg) studied earlier [32,34] which belong to the structural family of $Na_2Mg_5(MoO_4)_6$ [14].

3.2. The systems Ag_2MoO_4–MO–MoO_3 (M=Ca, Pb, Cd, Ni, Co, Mn)

In order to elucidate possibilities of the formation of double molybdates of silver and divalent metals with a different stoichiometry (or, more exactly, quaternary oxides), we investigated the phase formation in the ternary systems $Ag_2O-MO-MoO_3$ (M=Ca, Pb, Cd, Ni, Co, Mn). Since Ag_2O is stable in air below ~150°C only [43], this study was restricted, in fact, by the boundaries of the triangles $Ag_2MoO_4-MO-MoO_3$.

The phase formation in the binary systems $Ag_2MoO_4-MoO_3$ and $MO-MoO_3$ are described in detail in [35,37,38,44–47]. We confirmed the existence of $Ag_2Mo_2O_7$, $Ag_6Mo_{10}O_{33}$, $MMoO_4$ (M=Ca, Sr, Ba, Pb, Ni, Co, Mn) and Pb_2MoO_5. The compound Ca_3MoO_6 was not found, that agrees with the results of [38] about the stability of this compound in the narrow temperature range (1270–1370°C).

Taking into account the data on the phase formation in the side binary systems, we studied phase equilibria in the subsolidus area of the ternary systems $Ag_2MoO_4-MO-MoO_3$ systems and constructed their isothermal sections at 490°C. The results are given in Fig. 3.

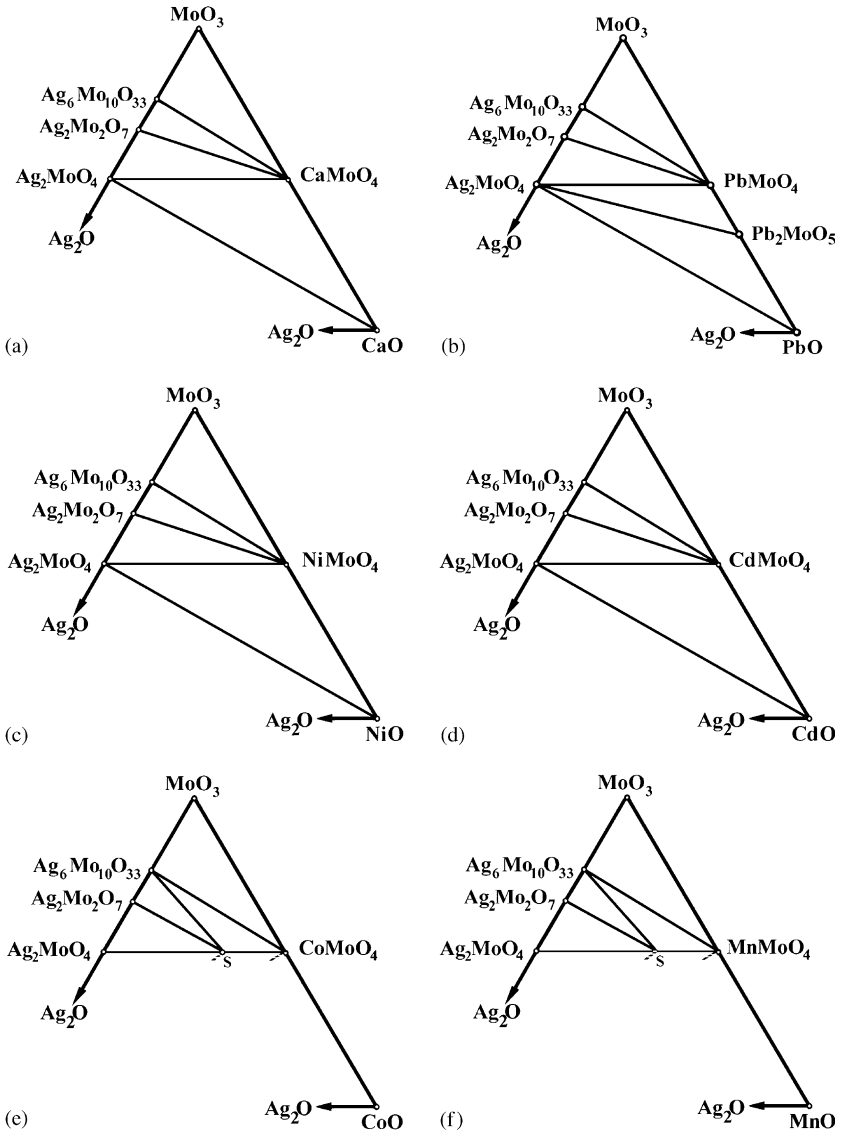

Fig. 3. Subsolidus phase relations in the systems $Ag_2MoO_4-MO-MoO_3$: (a) $Ag_2MoO_4-CaO-MoO_3$; (b) $Ag_2MoO_4-PbO-MoO_3$; (c) $Ag_2MoO_4-NiO-MoO_3$; (d) $Ag_2MoO_4-CdO-MoO_3$; (e) $Ag_2MoO_4-CoO-MoO_3$; (f) $Ag_2MoO_4-MnO-MoO_3$; S-$Ag_2M_2(MoO_4)_3$.

Triangulations of the ternary systems $Ag_2MoO_4-MO-MoO_3$ (M = Ca, Sr, Ba, Pb, Ni, Cd) are defined by quasibinary joins $Ag_2MoO_4-MMoO_4$, $Ag_2Mo_2O_7-MMoO_4$, $Ag_6Mo_{10}O_{33}-MMoO_4$, Ag_2MoO_4-MO (Figs. 3a and d). In the system with lead, the existence of another compound at the side PbO–MoO_3, Pb_2MoO_5, results in an increase in the number of the triangulating joins and the addition of the $Ag_2MoO_4-Pb_2MoO_5$ quasibinary section. No formation of any intermediate phases in the systems mentioned was observed.

The existence of double molybdates $Ag_2M_2(MoO_4)_3$ in the systems $Ag_2MoO_4-MO-MoO_3$ (M = Co, Mn) adds new quasibinary joins $Ag_2Mo_2O_7-Ag_2M_2(MoO_4)_3$ and $Ag_6Mo_{10}O_{33}-Ag_2M_2(MoO_4)_3$ to the triangulation nets (Figs. 3e and f). No other intermediate phases were found. The joins Ag_2MoO_4-MO (M = Co, Mn) are not quasibinary.

3.3. Crystal structures of $Ag_2M_2(MoO_4)_3$ (M=Co, Mn)

The unit cell parameters of triclinic $Ag_2M_2(MoO_4)_3$ (M = Co, Mn) indicated to the analogy of their structures to those of $Ag_2M_2(MoO_4)_3$ (M = Zn, Mg) [32,34] and therefore we used the coordinates of metal atoms taken from [34] as the starting structure model for $Ag_2Co_2(MoO_4)_3$. Refinement gave a good convergence ($R = 0.124$) and allowed to reveal the positions of 12 peaks of oxygen atoms on the difference map. After this the reliability factor fell to 0.098. At this stage, the analysis of cation-oxygen distances together with thermal factors was performed to find out the question

of possible statistical distribution (Ag, Co) and corresponding departure from stoichiometry. However, such evidence was not found. Further, going from isotropic to anisotropic thermal parameters and refining the site occupation factors for silver atoms with keeping the electrical neutrality condition, we decreased the reliability factors to $R(F) = 0.0313$, $wR(F^2) = 0.0792$. The refinement of the structure of LT-$Ag_2Mn_2(MoO_4)_3$ confirmed the same model of atomic arrangement. The positional and thermal parameters of $Ag_2M_2(MoO_4)_3$ (M = Co, Mn) are listed in Tables 2 and 3, respectively. Selected interatomic distances are given in Tables 4 and 5, respectively.

In the structures of $Ag_2M_2(MoO_4)_3$ (M = Co, Mn), three kinds of molybdenum atoms have common slightly deformed tetrahedral oxygen coordination with close average distances Mo–O 1.755–1.770 Å. The mean distances Mo–O in $Ag_2M_2(MoO_4)_3$ (M = Zn, Mg) [32,34] also fall in this interval. Two sorts of cobalt (manganese) atoms are octahedrally coordinated with longer distances Mn–O compared with corresponding those Co–O in agreement with a greater ionic radius of Mn^{2+}.

More interesting is to consider disorder, distribution over positions and environment of Ag^+ ions in the structures determined. Due to splitting the position Ag(1) → Ag(1A) + Ag(1B) with trigonal-bipyramidal coordination, we have two distinct coordination polyhedra around Ag(1A) and Ag(1B) which differ both the sets of separations Ag–O and their mean values. Preferable for occupation is the Ag(1A) site with more "roomy" environment. Note that occupancies of the sites Ag(1A) and Ag(1B) are slightly varied in $Ag_2M_2(MoO_4)_3$ (M = Mg, Co, Mn) in the above correspondence with differences in average distances Ag(1B)–O 2.35–2.39 Å rather than those Ag(1A)–O 2.412–4.419 Å. Atom Ag(2) has a somewhat deformed centrosymmetrical octahedral environment and mean distances Ag(2)–O 2.486–2.499 Å in $Ag_2M_2(MoO_4)_3$ (M = Co, Mn) are practically coincide with those in $Ag_2M_2(MoO_4)_3$ (M = Zn, Mg) [32,34].[1] Coordination of Ag(3A) is more irregular and ambiguous and very close to the environment of Ag(3) in $Ag_2Zn_2(MoO_4)_3$ [32]. In contradiction to data of [32], we established also partial filling an inversion center, Ag(3B), which close to the Ag(3A) site and has dumbbell coordination. The distribution of Ag^+ ions between the sites Ag(3A) and Ag(3B) are markedly varied in the row $Ag_2M_2(MoO_4)_3$ (M = Mg, Co, Mn). The maximum occupation of the Ag(3B) position is

Table 2
Positional and equivalent isotropic displacement parameters for $Ag_2Co_2(MoO_4)_3$

Atom	Occupancy	x	y	z	U_{eq} (Å^2)[a]
Mo(1)	1	0.62016(9)	0.09380(7)	0.33555(6)	0.0091(1)
Mo(2)	1	0.28751(9)	0.33861(7)	0.73916(6)	0.0094(1)
Mo(3)	1	0.09338(10)	0.24819(7)	0.13462(6)	0.0107(1)
Co(1)	1	0.5374(2)	0.1972(1)	0.0183(1)	0.0094(2)
Co(2)	1	0.1237(2)	0.0372(1)	0.3961(1)	0.0100(2)
Ag(1A)	0.78(6)	0.1697(9)	0.6563(9)	0.1581(9)	0.0245(8)
Ag(1B)	0.22[b]	0.1960(60)	0.6840(50)	0.1880(50)	0.039(4)
Ag(2)	1	1/2	1/2	1/2	0.0233(2)
Ag(3A)	0.45(1)	0.0058(4)	0.4702(7)	0.4307(13)	0.054(2)
Ag(3B)	0.10[c]	0	1/2	1/2	0.054(7)
O(1)	1	0.6959(9)	0.3133(6)	0.4260(6)	0.022(1)
O(2)	1	0.5798(8)	0.0544(6)	0.1489(5)	0.012(1)
O(3)	1	0.8265(8)	0.0248(6)	0.4194(5)	0.013(1)
O(4)	1	0.3876(8)	−0.0018(7)	0.3551(5)	0.019(1)
O(5)	1	0.0349(8)	0.2247(6)	0.7307(5)	0.016(1)
O(6)	1	0.3329(9)	0.5569(6)	0.8214(5)	0.020(1)
O(7)	1	0.4793(8)	0.2805(7)	0.8467(5)	0.018(1)
O(8)	1	0.2802(8)	0.2905(6)	0.5562(5)	0.015(1)
O(9)	1	−0.1570(8)	0.2269(6)	0.0161(5)	0.018(1)
O(10)	1	0.2502(9)	0.1861(7)	0.0359(6)	0.022(1)
O(11)	1	0.0628(9)	0.1304(7)	0.2423(6)	0.025(1)
O(12)	1	0.2261(10)	0.4615(7)	0.2552(6)	0.031(1)

[a] U_{eq} is defined as one third of the trace of the orthogonalized U_{ij} tensor.
[b] s.o.f. of Ag(1B) was supposed as 1−s.o.f. [Ag(1A)].
[c] s.o.f. of Ag(3B) was supposed as 1−2s.o.f. [Ag(3A)].

Table 3
Positional and equivalent isotropic displacement parameters for LT-$Ag_2Mn_2(MoO_4)_3$

Atom	Occupancy	x	y	z	U_{eq} (Å^2)[a]
Mo(1)	1	0.62092(5)	0.09402(4)	0.33505(3)	0.0112(1)
Mo(2)	1	0.28423(5)	0.33986(4)	0.73472(3)	0.0120(1)
Mo(3)	1	0.09509(5)	0.25662(4)	0.13407(3)	0.0136(1)
Mn(1)	1	0.53958(9)	0.20397(7)	0.01912(6)	0.0124(1)
Mn(2)	1	0.12566(9)	0.04030(8)	0.39167(6)	0.0125(1)
Ag(1A)	0.77(4)	0.1839(5)	0.6675(5)	0.1764(5)	0.0291(5)
Ag(1B)	0.23[b]	0.1970(20)	0.6837(16)	0.1970(20)	0.042(2)
Ag(2)	1	1/2	1/2	1/2	0.0264(1)
Ag(3A)	0.30(1)	0.0085(5)	0.4684(5)	0.4329(4)	0.042(1)
Ag(3B)	0.40[c]	0	1/2	1/2	0.169(7)
O(1)	1	0.6963(6)	0.3106(4)	0.4259(4)	0.0261(7)
O(2)	1	0.5777(5)	0.0526(4)	0.1501(3)	0.0153(5)
O(3)	1	0.8228(5)	0.0232(4)	0.4163(3)	0.0149(5)
O(4)	1	0.3887(5)	−0.0022(4)	0.3532(4)	0.0200(6)
O(5)	1	0.0371(5)	0.2283(4)	0.7270(3)	0.0182(5)
O(6)	1	0.3241(6)	0.5527(4)	0.8135(4)	0.0255(7)
O(7)	1	0.4785(5)	0.2846(5)	0.8408(4)	0.0219(6)
O(8)	1	0.2799(5)	0.2949(4)	0.5555(3)	0.0193(6)
O(9)	1	0.1493(5)	0.7587(5)	−0.0153(4)	0.0210(6)
O(10)	1	0.0371(5)	0.2283(4)	0.7270(3)	0.0324(9)
O(11)	1	0.3241(6)	0.5527(4)	0.8135(4)	0.0322(9)
O(12)	1	0.2302(8)	0.4635(5)	0.2608(5)	0.0426(12)

[a] U_{eq} is defined as one third of the trace of the orthogonalized U_{ij} tensor.
[b] s.o.f. of Ag(1B) was supposed as 1−s.o.f. [Ag(1A)].
[c] s.o.f. of Ag(3B) was supposed as 1—2s.o.f. [Ag(3A)].

[1] The numeration of atoms in the structures of $Ag_2M_2(MoO_4)_3$ (M = Zn, Mg, Co, Mn) are the same, but $Ag_2Zn_2(MoO_4)_3$ has different crystallographic setting.

Table 4
Selected interatomic distances (Å) in structure of $Ag_2Co_2(MoO_4)_3$

$Mo(1)O_4$ tetrahedron		$Mo(2)O_4$ tetrahedron		$Mo(3)O_4$ tetrahedron	
Mo(1)–O(1)	1.731(5)	Mo(2)–O(6)	1.745(5)	Mo(3)–O(12)	1.742(5)
Mo(1)–O(4)	1.733(5)	Mo(2)–O(5)	1.772(5)	Mo(3)–O(11)	1.746(5)
Mo(1)–O(2)	1.777(4)	Mo(2)–O(7)	1.779(5)	Mo(3)–O(10)	1.751(6)
Mo(1)–O(3)	1.807(5)	Mo(2)–O(8)	1.785(5)	Mo(3)–O(9)	1.780(5)
⟨Mo(1)–O⟩	1.762	⟨Mo(2)–O⟩	1.770	⟨Mo(3)–O⟩	1.755
$Co(1)O_6$ octahedron		$Co(2)O_6$ octahedron		$Ag(1A)O_5$ trigonal	
Co(1)–O(10)	2.045(6)	Co(2)–O(11)	1.986(5)	Bipyramid	
Co(1)–O(6)[a]	2.071(5)	Co(2)–O(4)	2.079(6)	Ag(1A)–O(12)	2.280(7)
Co(1)–O(7)[b]	2.088(5)	Co(2)–O(5)[e]	2.092(5)	Ag(1A)–O(5)[h]	2.300(8)
Co(1)–O(9)[c]	2.095(6)	Co(2)–O(3)[f]	2.095(5)	Ag(1A)–O(9)[i]	2.311(6)
Co(1)–O(2)	2.107(4)	Co(2)–O(8)	2.118(5)	Ag(1A)–O(7)[a]	2.399(7)
Co(1)–O(2)[d]	2.136(4)	Co(2)–O(3)[g]	2.134(5)	Ag(1A)–O(4)[j]	2.805(10)
⟨Co(1)–O⟩	2.090	⟨Co(2)–O⟩	2.084	⟨Ag(1A)–O⟩	2.419
$Ag(1B)O_5$ trigonal		$Ag(2)O_6$ octahedron		$Ag(3A)O_7$ polyhedron	
Bipyramid		Ag(2)–O(8)	$2.410(5)\times 2$	Ag(3A)–O(1)[a]	2.213(7)
Ag(1B)–O(5)[h]	2.21(2)	Ag(2)–O(1)	$2.446(6)\times 2$	Ag(3A)–O(1)[g]	2.248(7)
Ag(1B)–O(12)	2.29(2)	Ag(2)–O(12)	$2.601(6)\times 2$	Ag(3A)–O(12)	2.661(13)
Ag(1B)–O(7)[a]	2.35(2)	⟨Ag(2)–O⟩	2.486	Ag(3A)–O(6)[h]	2.919(9)
Ag(1B)–O(9)[i]	2.42(3)			Ag(3A)–O(8)	3.030(6)
Ag(1B)–O(4)[j]	2.54(5)	$Ag(3B)O_2$ dumbbell		Ag(3A)–O(11)	3.197(11)
⟨Ag(1B)–O⟩	2.36	Ag(3B)–O(1)[a]	$2.119(6)\times 2$	Ag(3A)–O(8)[h]	3.219(7)
Shortest non-bonded contacts					
Ag(3A)–Ag(3B)	0.70(1)	Ag(3A)–Ag(3A)[h]	1.39(3)	Ag(2)–Ag(3A)[a]	3.266(3)

Note. Symmetry code: [a] $-x+1, -y+1, -z+1$; [b] $x, y, z-1$; [c] $x+1, y, z$; [d] $-x+1, -y, -z$; [e] $-x, -y, -z+1$; [f] $-x+1, -y, -z+1$; [g] $x-1, y, z$; [h] $-x, -y+1, -z+1$; [i] $-x, -y+1, -z$; [j] $x, y+1, z$.

Table 5
Selected interatomic distances (Å) in structure of LT-$Ag_2Mn_2(MoO_4)_3$

$Mo(1)O_4$ tetrahedron		$Mo(2)O_4$ tetrahedron		$Mo(3)O_4$ tetrahedron	
Mo(1)–O(1)	1.748(4)	Mo(2)–O(6)	1.745(3)	Mo(3)–O(11)	1.737(4)
Mo(1)–O(4)	1.753(3)	Mo(2)–O(5)	1.764(3)	Mo(3)–O(10)	1.746(4)
Mo(1)–O(2)	1.776(3)	Mo(2)–O(7)	1.779(3)	Mo(3)–O(12)	1.761(4)
Mo(1)–O(3)	1.799(3)	Mo(2)–O(8)	1.782(3)	Mo(3)–O(9)	1.781(3)
⟨Mo(1)–O⟩	1.769	⟨Mo(2)–O⟩	1.768	⟨Mo(3)–O⟩	1.756
$Mn(1)O_6$ octahedron		$Mn(2)O_6$ octahedron		$Ag(1A)O_5$ trigonal	
Mn(1)–O(10)	2.106(4)	Mn(2)–O(11)	2.048(4)	bipyramid	
Mn(1)–O(6)[a]	2.131(3)	Mn(2)–O(4)	2.107(3)	Ag(1A)–O(12)	2.283(5)
Mn(1)–O(7)[b]	2.151(3)	Mn(2)–O(5)[e]	2.179(3)	Ag(1A)–O(5)[h]	2.310(4)
Mn(1)–O(9)[c]	2.165(3)	Mn(2)–O(8)	2.187(3)	Ag(1A)–O(9)[i]	2.338(4)
Mn(1)–O(2)	2.185(3)	Mn(2)–O(3)[f]	2.192(3)	Ag(1A)–O(7)[a]	2.396(4)
Mn(1)–O(2)[d]	2.226(3)	Mn(2)–O(3)[g]	2.207(3)	Ag(1A)–O(4)[j]	2.735(6)
⟨Mn(1)–O⟩	2.161	⟨Mn(2)–O⟩	2.153	⟨Ag(1A)–O⟩	2.412
$Ag(1B)O_5$ trigonal		$Ag(2)O_6$ octahedron		$Ag(3A)O_7$ polyhedron	
Bipyramid		Ag(2)–O(8)	$2.416(3)\times 2$	Ag(3A)–O(1)[a]	2.255(5)
Ag(1B)–O(5)[h]	2.23(1)	Ag(2)–O(1)	$2.512(4)\times 2$	Ag(3A)–O(1)[g]	2.291(5)
Ag(1B)–O(12)	2.28(1)	Ag(2)–O(12)	$2.570(4)\times 2$	Ag(3A)–O(12)	2.686(6)
Ag(1B)–O(7)[a]	2.41(1)	⟨Ag(2)–O⟩	2.499	Ag(3A)–O(6)[h]	2.897(6)
Ag(1B)–O(9)[i]	2.45(2)			Ag(3A)–O(8)	2.986(6)
Ag(1B)–O(4)[j]	2.57(2)	$Ag(3B)O_2$ dumbbell		Ag(3A)–O(8)[h]	3.263(6)
⟨Ag(1B)–O⟩	2.39	Ag(3B)–O(1)[a]	$2.163(4)\times 2$	Ag(3A)–O(11)	3.274(6)
Shortest non-bonded contacts					
Ag(3A)–Ag(3B)	0.698(3)	Ag(3A)–Ag(3A)[h]	1.396(6)	Ag(2)–Ag(3A)[a]	3.288(3)

Note. Symmetry code: [a] $-x+1, -y+1, -z+1$; [b] $x, y, z-1$; [c] $x+1, y, z$; [d] $-x+1, -y, -z$; [e] $-x, -y, -z+1$; [f] $-x+1, -y, -z+1$; [g] $x-1, y, z$; [h] $-x, -y+1, -z+1$; [i] $-x, -y+1, -z$; [j] $x, y+1, z$.

reached for manganese derivative where we look the longest bonds Ag(3B)–O 2.163(4) Å.

The authors of [32] suggested for the structure of $Ag_2Zn_2(MoO_4)_3$ two other models of silver disorder. In the first, more simple model, there are the unsplitted Ag(1) position and the site Ag(3)≡Ag(3A). In the second, more complicated model, the Ag(1) position was splitted into five sites and the Ag(3) site gives three positions. We proposed for the structures of $Ag_2M_2(MoO_4)_3$ (M = Mg, Co, Mn) another, sort of intermediate and more realistic, model of silver disorder which was found to be practically invariable for the three cases. On the other hand, for isotypical $Ag_{0.5}Cu_3^{2+}V_{0.5}Mo_{0.5}O_{12}$ [48], it is found the site Ag(2) site to split while the position Ag(1) occupied by Cu^{2+} is not splitted. Apparently, the modes of a low-charged cation disorder in the structure type depend on compound composition. In addition, we guess that some differences in the cation disorder models may be connected with discrepancies in interpretation of electron density maps and other details of structure refinement.

The projections of the structure of $Ag_2Co_2(MoO_4)_3$ in two different orientations are shown in Fig. 4. The structure may be represented as a mixed framework of MoO_4 tetrahedra and pairs of CoO_6 octahedra sharing common edges. Silver atoms are located in the voids forming infinite channels running along the a direction. Note that the architecture of the structures discussed was repeatedly described in detail [14,32,49] and no need to do this again.

From the above results and paying no regard to possible peculiarities of silver disorder in $Ag_2Zn_2(MoO_4)_3$ [32], we can conclude that all the phases $Ag_2M_2(MoO_4)_3$ (M = Zn, Mg, Co, Mn) are isostructural and show only small variations in the unit cell parameters in accordance with ionic radii (Table 6). All the studied compounds prove to be stoichiometric though we and authors of [13] admit possibility of a little departure of their compositions to some deficiency of silver content to give general formula $Ag_{2-2x}M_{2+x}(MoO_4)_3$.

Rather more serious discrepancies in compositions and structures occur compared with sodium-containing double molybdates $Na_2Mg_5(MoO_4)_6$ [14] and $Na_{0.5}Zn_{2.75}(MoO_4)_3$ [49] where the departures from stoichiometry are significant. This fact may be explained by a greater size of Ag^+ ion in comparison with ionic radius of Na^+ and all the more M^{2+} that essentially blocks the isomorphous substitution (Ag^+, M^{2+}) in the key position with trigonal–bipyramidal coordination. We showed [50] that in the sodium-containing double molybdates, the positions Ag(1), Ag(2), and Ag(3) (no splitting takes into consideration) correspond to the sites completely occupied by (Na^+, M^{2+}) and Na^+ and the defect position of (Na^+, □), respectively. Unfortunately, the authors of [14,49] missed the latter position in the course of their structure determinations that strongly influences on the results. Nevertheless, though we may not yet to consider the compositions of all discussed compounds as determined finally, close similarity in the structure permits to write their general formula as $A^+_{2-2x}M^{2+}_{2+x}(MoO_4)_3$ (A = Na, Ag; $0 \leqslant x \leqslant 0.5$) where the compositions of sodium-containing phases approach to the upper limit while those of silver-containing ones close to the lower limit.

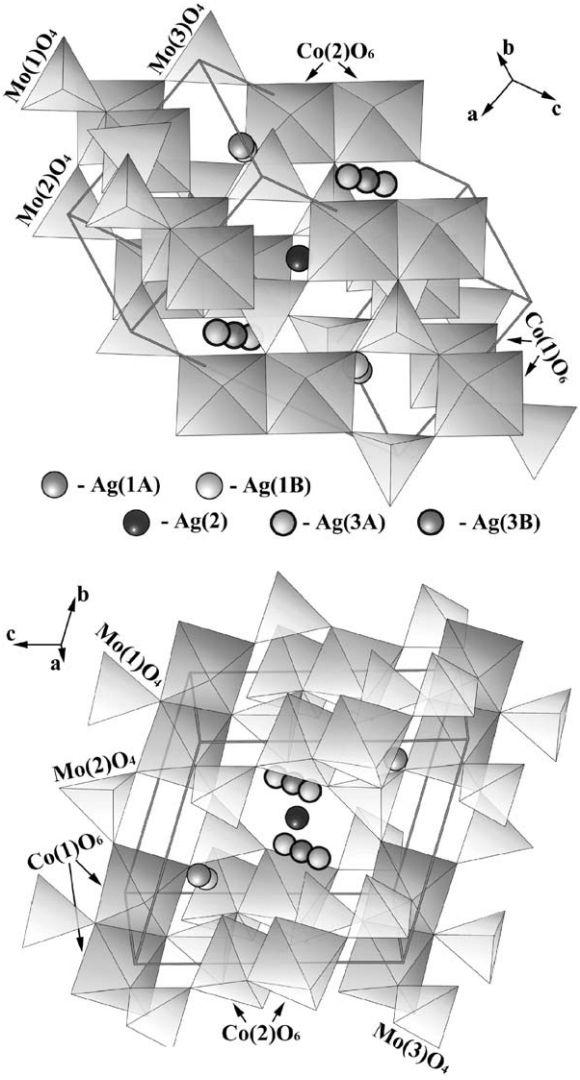

Fig. 4. Two projections of the $Ag_2Co_2(MoO_4)_3$ structure.

The interesting peculiarity of $Ag_2Mn_2(MoO_4)_3$ is the LT→HT phase transition to high-temperature modification accompanying only some broadening the XRD pattern lines of the quenched samples. The same phenomenon was observed for $Ag_2Mg_2(MoO_4)_3$ [32]. We admit that may be associated with sharp raising the silver disorder, which is already characteristic for a part of Ag^+ ions in the both structures of the low-temperature forms. Possible ways of further disordering

Table 6
Unit cell parameters for $Ag_2M_2(MoO_4)_3$ (M = Zn, Mg, Co, Mn) in compatible settings

Compound	Unit cell parameters			V (Å^3)	Reference
	a (Å); α (deg)	b (Å); β (deg)	c (Å); γ (deg)		
$Ag_2Zn_2(MoO_4)_3$[a]	6.992	8.712	10.277	542.8	[32]
	107.22	105.12	103.73		
LT-$Ag_2Mg_2(MoO_4)_3$	6.978	8.715	10.294	541.4	[34]
	107.56	105.11	103.68		
$Ag_2Co_2(MoO_4)_3$	6.989	8.738	10.295	541.8	This work
	107.67	105.28	103.87		
LT-$Ag_2Mn_2(MoO_4)_3$	7.093	8.878	10.415	566.9	This work
	106.86	105.84	103.77		

[a] Lattice parameters are converted from original setting by matrix −100/010/10−1.

are changes in the balances of the occupation factors of the sites Ag(1A) and Ag(1B), Ag(3A) and Ag(3B), respectively, and, in addition, splitting the position Ag(2) into two off-center sites as in $Ag_{0.5}Cu_3^{2+}V_{0.5}Mo_{0.5}O_{12}$ [48]. A possible further silver redistribution in high-temperature HT–$Ag_2M_2(MoO_4)_3$ (M = Mg, Mn) could result in a more equable occupation of the structure channels by Ag^+ ions and give rise to higher their mobility. If it is so, the phase transitions in $Ag_2M_2(MoO_4)_3$ (M = Mg, Mn) may have superionic character that attracts interest to the electrical conductivity measurements of these compounds. The results of corresponding experiments will be published elsewhere.

References

[1] I.N. Belyaev, Zh. Neorg. Khim. 6 (1961) 1178 (in Russian).
[2] I.N. Belyaev, N.N. Chikova, Zh. Neorg. Khim. 9 (1964) 2754 (in Russian).
[3] J.A. Ibers, G.W. Smith, Acta Crystallogr. 17 (1964) 190.
[4] L.G. Van Uitert, R.C. Sherwood, H.J. Williams, J.J. Rubin, W.A. Bonner, J. Phys. Chem. Solids. 25 (1964) 1447.
[5] R.F. Klevtsova, S.A. Magarill, Kristallografiya 15 (1970) 710 (in Russian).
[6] V.K. Trunov, Zh. Neorg. Khim. 16 (1971) 553 (in Russian).
[7] L. Katz, A. Kasenally, L. Kihlborg, Acta crystallogr. B 27 (1971) 2071.
[8] C. Gicquel, M. Mayer, G. Perez, R. Bouaziz, C. R. Acad. Sci. Paris C 275 (1972) 265.
[9] V.A. Efremov, V.K. Trunov, Zh. Neorg. Khim. 17 (1972) 2034 (in Russian).
[10] V.A. Efremov, V.K. Trunov, Zh. Neorg. Khim. 20 (1975) 2200 (in Russian).
[11] C. Gicquel-Mayer, G. Perez, Rev. Chim. Miner. 12 (1975) 537.
[12] M. Ozima, S. Sato, T. Zoltai, Acta Crystallogr. B 33 (1977) 2175.
[13] P.V. Klevtsov, V.G. Kim, R.F. Klevtsova, Kristallografiya 25 (1980) 301 (in Russian).
[14] P.V. Klevtsov, V.G. Kim, R.F. Klevtsova, Kristallografiya 25 (1980) 1148 (in Russian).
[15] T. Machej, J. Ziolkowski, J. Solid State Chem. 31 (1980) 135.
[16] M. Müller, B.O. Hildmann, T. Hahn, Z. Kristallogr. 174 (1986) 152.
[17] S.I. Arkhincheeva, Zh.G. Bazarova, M.V. Mokhosoev, Dokl. Akad. Nauk SSSR 290 (1986) 120 (in Russian).
[18] G.D. Tsyrenova, Zh.G. Bazarova, M.V. Mokhosoev, Dokl. Akad. Nauk SSSR 294 (1987) 387 (in Russian).
[19] Zh.G. Bazarova, G.D. Tsyrenova, S.I. Arkhincheeva, M.V. Mokhosoev, M.N. Ivanova, Zh. Neorg. Khim. 33 (1988) 449 (in Russian).
[20] S.F. Solodovnikov, R.F. Klevtsova, P.V. Klevtsov, Zh. Strukt. Khim. 35 (1994) 145 (in Russian).
[21] S.F. Solodovnikov, Z.A. Solodovnikova, P.V. Klevtsov, E.S. Zolotova, Zh. Neorg. Khim. 40 (1995) 223 (in Russian).
[22] H. Szillat, Hk. Müller-Bushbaum, Z. Naturforsch. 50b (1995) 247.
[23] E.F. Dudnik, I.E. Mnushkina, Fiz. Tverd. Tela 18 (1976) 3150 (in Russian).
[24] E.F. Dudnik, I.E. Mnushkina, Ukr. Fiz. Zh. 22 (1977) 1737.
[25] N.I. Korosteleva, V.I. Kovalenko, E.A. Ukshe, Izv. Akad. Nauk SSSR. Neorg. Mater. 17 (1981) 741 (in Russian).
[26] J. Grins, M. Nygren, Solid State Ionics. 9–10 (1983) 859.
[27] G.D. Tsyrenova, Zh.G. Bazarova, M.V. Mokhosoev, Zh. Neorg. Khim. 33 (1988) 452 (in Russian).
[28] A.L. Kruglyashov, E.M. Skou, Solid State Ionics. 28–30 (1988) 233.
[29] P.V. Klevtsov, V.G. Kim, A.I. Kruglik, R.F. Klevtsova, Kristallografiya 34 (1989) 1475 (in Russian).
[30] A.K. Ivanov-Shits, A.V. Nistyuk, N.G. Chaban, Neorg. Mater. 15 (1999) 891 (in Russian).
[31] G.D. Tsyrenova, S.F. Solodovnikov, E.S. Zolotova, B.A. Tsybikova, Zh.G. Bazarova, Zh. Neorg. Khim. 45 (2000) 109 (in Russian).
[32] C. Gicquel-Mayer, M. Mayer, G. Perez, Acta Crystallogr. B 37 (1981) 1035.
[33] G.D. Tsyrenova, S.S. Gypylova, S.F. Solodovnikov, E.S. Zolotova, Zh. Neorg. Khim. 45 (2000) 2057 (in Russian).
[34] G.D. Tsyrenova, S.F. Solodovnikov, E.G. Khaikina, E.T. Khobrakova, Zh. Neorg. Khim. 46 (2001) 2066 (in Russian).
[35] R. Kohlmuller, J.-P. Faurie, Bull. Soc. Chim. Fr. 11 (1968) 4379.
[36] Powder Diffraction File, ICDD, No. 08-0474.
[37] P.S. Mamykin, N.A. Batrakov, Trudy Ural'skogo Polytekhnicheskogo Instituta, Proceedings of Ural Polytechnic Institute, Issue 150, UPI, Sverdlovsk, 1966, p. 101 (in Russian).
[38] V.M. Zhukovsky, E.V. Tkachenko, Fizicheskaya Khimiya Okislov Metallov, Physical Chemistry of Metal Oxides, Nauka, Moscow, 1981 (in Russian).
[39] A.M. Zakharov, Fazovye diagrammy dvoinykh i troinykh sistem, Phase diagrams of binary and ternary systems, Metallurgiya, Moscow, 1978 (in Russian).

[40] L.G. Akselrud, P.J. Zavalij, Yu.N. Gryn, V.K. Pecharskii, B. Baumgartner, E. Wolfel, Mater. Sci. Forum 133–136 (1993) 335.
[41] G.M. Sheldrick, SHELX-97, Release 97-2, University of Goettingen, 1997.
[42] A.W. Sleight, Inorg. Chem. 7 (1968) 1672.
[43] J. Assal, B. Hallsted, L.J. Gauckler, J. Am. Ceram. Soc. 80 (1997) 3054.
[44] B.M. Gatehouse, P. Leverett, Chem. Commun. 19 (1969) 1093.
[45] B.M. Gatehouse, P. Leverett, J. Solid State Chem. 1 (1970) 484.
[46] B.M. Gatehouse, P. Leverett, J. Chem. Soc. Dalton Trans. 14 (1976) 1316.
[47] N.N. Shevchenko, L.N. Lykova, L.M. Kovba, Zh. Neorg. Khim. 19 (1974) 971 (in Russian).
[48] H. Szillat, Hk. Müller-Buschbaum, Z. Naturforsch. B 50 (1995) 879.
[49] C. Gicquel-Mayer, M. Mayer, Rev. Chim. Miner. 19 (1982) 91.
[50] S.F. Solodovnikov, D. Sc. (Chemistry) thesis, Institute of Inorganic Chemistry, SB RAS. Novosibirsk, Russia, 2000.